

AD

TECHNICAL REPORT ARCCB-TR-01019

**PROPERTIES OF THICK SPUTTERED TANTALUM
USED FOR PROTECTIVE GUN TUBE COATINGS**

**DEAN W. MATSON
EDWIN D. McCLANAHAN
SABRINA L. LEE
DONALD WINDOVER**

OCTOBER 2001



**US ARMY ARMAMENT RESEARCH,
DEVELOPMENT AND ENGINEERING CENTER
CLOSE COMBAT ARMAMENTS CENTER
BENÉT LABORATORIES
WATERVLIET, N.Y. 12189-4050**



DISTRIBUTION STATEMENT A
Approved for Public Release
Distribution Unlimited

20011105 050

DISCLAIMER

The findings in this report are not to be construed as an official Department of the Army position unless so designated by other authorized documents.

The use of trade name(s) and/or manufacturer(s) does not constitute an official endorsement or approval.

DESTRUCTION NOTICE

For classified documents, follow the procedures in DoD 5200.22-M, Industrial Security Manual, Section II-19, or DoD 5200.1-R, Information Security Program Regulation, Chapter IX.

For unclassified, limited documents, destroy by any method that will prevent disclosure of contents or reconstruction of the document.

For unclassified, unlimited documents, destroy when the report is no longer needed. Do not return it to the originator.

REPORT DOCUMENTATION PAGE

Form Approved
OMB No. 0704-0188

Public reporting burden for this collection of information is estimated to average 1 hour per response, including the time for reviewing instructions, searching existing data sources, gathering and maintaining the data needed, and completing and reviewing the collection of information. Send comments regarding this burden estimate or any other aspect of this collection of information, including suggestions for reducing this burden, to Washington Headquarters Services, Directorate for Information Operations and Reports, 1215 Jefferson Davis Highway, Suite 1204, Arlington, VA 22202-4302, and to the Office of Management and Budget, Paperwork Reduction Project (0704-0188), Washington, DC 20503.

1. AGENCY USE ONLY (Leave blank)		2. REPORT DATE October 2001	3. REPORT TYPE AND DATES COVERED Final	
4. TITLE AND SUBTITLE PROPERTIES OF THICK SPUTTERED TANTALUM USED FOR PROTECTIVE GUN TUBE COATINGS			5. FUNDING NUMBERS AMCMS No. 7780.45.E251.200	
6. AUTHOR(S) Dean W. Matson (Pacific Northwest National Laboratory, Richland, WA), Edwin D. McClanahan (Pacific Northwest), Sabrina L. Lee, and Donald Windover (Benet and RPI, Troy, NY)				
7. PERFORMING ORGANIZATION NAME(S) AND ADDRESS(ES) U.S. Army ARDEC Benet Laboratories, AMSTA-AR-CCB-O Watervliet, NY 12189-4050			8. PERFORMING ORGANIZATION REPORT NUMBER ARCCB-TR-01019	
9. SPONSORING / MONITORING AGENCY NAME(S) AND ADDRESS(ES) U.S. Army ARDEC Close Combat Armaments Center Picatinny Arsenal, NJ 07806-5000			10. SPONSORING / MONITORING AGENCY REPORT NUMBER	
11. SUPPLEMENTARY NOTES Presented at the International Conference on Metallurgical Coatings and Thin Films, San Diego, CA, 30 April to 4 May 2001. Published in <i>Metallurgical Coatings and Thin Films</i> .				
12a. DISTRIBUTION / AVAILABILITY STATEMENT Approved for public release; distribution unlimited.			12b. DISTRIBUTION CODE	
13. ABSTRACT (Maximum 200 words) Thick tantalum coatings were deposited on the bore surfaces of 25-mm inner diameter cylindrical gun steel substrates using a high-rate triode-sputtering apparatus. Sputtering parameters affecting the tantalum phase and microstructure were investigated. Prior work has indicated that the sputtering gas species and substrate temperature during deposition affect the characteristics of the tantalum coatings. In the work presented here, we report on experimental studies aimed at evaluating additional phase and microstructural effects resulting from changes in sputtering gas species and substrate bias during the deposit. Tantalum deposits of 75 to 140 μm thickness were evaluated using x-ray diffraction, optical microscopy, and microindentation hardness measurements. Coatings deposited using krypton gas, a 200°C substrate temperature, and 3.5 mTorr gas pressure also showed little variation when deposited at substrate biases ranging from 50 to 150 V. However, the tantalum coatings produced under similar conditions with an unbiased (floating) substrate were found to be the beta phase of the material and had a columnar microstructure. Beta-phase tantalum was produced at low substrate biases (≤50 V) when using xenon as the sputtering gas. Both phase and microstructure of the tantalum coating could be altered in mid-run by adjusting the sputtering parameters and appeared independent of the phase and microstructure of the underlying coating.				
14. SUBJECT TERMS Tantalum, Phase, Microstructure, High-Rate Sputtering, Sputtering Gas, Sputtering Bias			15. NUMBER OF PAGES 16	
			16. PRICE CODE	
17. SECURITY CLASSIFICATION OF REPORT	18. SECURITY CLASSIFICATION OF THIS PAGE	19. SECURITY CLASSIFICATION OF ABSTRACT	20. LIMITATION OF ABSTRACT	
UNCLASSIFIED	UNCLASSIFIED	UNCLASSIFIED		

TABLE OF CONTENTS

	<u>Page</u>
ACKNOWLEDGEMENTS	iii
INTRODUCTION.....	1
EXPERIMENTAL METHOD	2
Coating Conditions.....	2
Coating Characterization.....	3
RESULTS AND DISCUSSION	4
CONCLUSIONS AND FUTURE WORK	6
REFERENCES	8

TABLES

1. Deposition Conditions and Properties of Thick Tantalum Coatings Produced Using a Cylindrical Triode-Sputtering Apparatus 3

LIST OF ILLUSTRATIONS

1. Photomicrographs of cross-sectioned and acid-etched tantalum coatings produced in the cylindrical triode-sputtering apparatus with a 200°C substrate temperature and -100 V substrate bias using (a) argon (#121), (b) krypton (#132), and (c) xenon (#125) sputtering gases..... 9
2. Photomicrograph of a cross-sectioned and acid-etched tantalum coating (sample #147) produced by sequential deposition with xenon and argon sputtering gases at ~165°C substrate temperature and a -100 V substrate bias 10
3. Photomicrograph and x-ray diffraction pattern of a tantalum coating (sample #146) produced using xenon gas, a 100°C substrate temperature, and -100 V substrate bias ... 10
4. Photomicrographs of tantalum coatings produced using krypton sputtering gas, a 200°C substrate temperature, and various substrate biases including (a) floating (#150), (b) -50 V (#155), (c) -100 V (#161), and (d) -150 V (#152) 11
5. Photomicrograph of a sputtered tantalum sample (#163) produced using krypton sputtering gas, a 200°C substrate temperature, and a stepped substrate bias (initially unbiased, -100 V in the outer layer)..... 12

6. Photomicrograph of a cross-sectioned, sputtered tantalum coating (sample #158) produced using xenon gas, a 200°C substrate temperature, and various substrate biases (0 to -50 V for the deposit closest to the steel interface and -100 V for the outer layer) 13

ACKNOWLEDGEMENTS

The Strategic Environmental Research and Development Program (SERDP) provided funding to Pacific Northwest Laboratory and U.S. Army ARDEC- Benét Laboratories for this research project. Pacific Northwest Laboratory is operated by the U.S. Department of Energy, Battelle Memorial Institute, under Contract DE-AC06-76RLO 1830.

INTRODUCTION

Tantalum is being considered as a replacement for chromium in use as a protective bore coating material for medium and large caliber military gun tubes. Tantalum, in its common bulk body-centered-cubic form (bcc phase), is highly refractory (mp = 2996°C versus 1860°C for chromium) and has a relatively low thermal conductivity (57 W/m°C versus 91 W/m°C for chromium at 20°C). In addition, tantalum is chemically resistant to corrosive propellant gases and the bcc phase is much more ductile than chromium, making it far less susceptible to crack formation causing coating failure in gun tube applications. Tantalum is also not plagued by the health and environmental issues associated with the plating baths used for application of the chromium coatings.

One approach being evaluated for depositing tantalum coatings on gun bore surfaces is sputtering (refs 1-4). However, besides the desirable bcc form, vapor-deposited tantalum is often found to exist in the form of a tetragonal phase commonly referred to as beta-tantalum (refs 5-7). The beta phase is metastable, reverting to the bcc form at temperatures above 750°C, and is much harder and more brittle than the bcc phase. Typical Knoop microhardness values for beta-tantalum are greater than 900 versus Knoop values of 300 to 400 for bcc tantalum (ref 2). These properties make beta-tantalum more susceptible to crack formation and failure, and hence less desirable for bore coating applications where high shear forces are present. Often mixed-phase deposits are observed in thick sputtered tantalum (refs 1,2).

Because of the importance of tantalum as an electronic material, and because the bcc and beta forms have distinct electrical properties, conditions for the preferred nucleation of the two phases in thin-film form have been extensively studied (refs 8-14). Unfortunately, extrapolation of those thin-film deposition conditions to the high-rate requirements and relatively thick coatings needed for gun bore applications (typically $\geq 75 \mu\text{m}$) are not necessarily straightforward. Additional complications arise from the necessary use of steel as the substrate material, the cylindrical geometry, and thermal and stress cycling to which the coatings are subjected under use in gun tube applications.

This report presents the results of the latest studies undertaken at the Pacific Northwest National Laboratory in which we have evaluated the phase distribution and microstructure in thick tantalum films produced using a cylindrical-geometry, high-rate triode-sputtering apparatus. In prior papers, we have described the use of a niobium underlayer to promote bcc formation (ref 1), and have presented preliminary results relating the effects of sputtering gas species and substrate temperature to the tantalum phase produced directly on steel substrates (ref 2). This report presents additional results of studies evaluating these variables, as well as preliminary results on the effects of sputtering bias on both the tantalum phase and coating microstructure.

EXPERIMENTAL METHOD

Coating Conditions

Thick tantalum coatings (80 to 150 μm) were deposited on the inner surfaces of bored-through 4340 steel right circular cylinders (25-mm inner diameter, 42-mm outer diameter, 77-mm long) using a high-rate, cylindrical geometry sputtering apparatus described in a prior publication (ref 2). Noteworthy components of the system are briefly summarized. A tantalum ribbon auxiliary cathode mounted in the base below the steel substrate cylinder was used as an electron source to support a low-pressure plasma in the system. The lid of the apparatus, at the opposite end of the cylinder, acted as the anode. The steel substrate cylinders were slip-fit into a water-cooled aluminum jacket that also served as the outer vacuum chamber. The outside diameters of the steel substrate cylinders were precision machined so that the substrate temperature during sputter deposition was controlled by the difference between the outer diameter of the substrate cylinder and the inner diameter of the aluminum jacket.

The substrate cylinder temperature was limited as it was heated (due to plasma exposure and coating process effects) and achieved a thermal equilibrium with the water-cooled aluminum. Substrate temperatures were monitored by using two spring-loaded, metal-sheathed thermocouples mounted through o-ring sealed feed-throughs in the aluminum jacket. Thermocouple tips were inserted into small wells machined into the outer surface of the steel substrate cylinders. A water-cooled tantalum sputtering target assembly consisted of a 10-cm length of heavy-walled tantalum tubing (9.5-mm outer diameter) brazed to stainless steel tubing extensions. O-ring sealed fittings at the top and bottom of the vacuum chamber centered the target assembly along the longitudinal axis of the substrate tube. These fittings also allowed cooling water connections to be made to the target externally, thus permitting movement of the tantalum section into and out of the sputtering position by translating the target assembly along its axis.

Coating runs included a pre-run system plasma bake-out at full plasma power (60 A plasma current using krypton gas for one hour) to minimize background gas contamination. After the pre-run bakeout, the system was allowed to cool overnight. During the coating phase of the run on the following day, the system was raised to full plasma power over a 30-minute period with the sputtering gas to be used for that run. A series of plasma etches was performed on all components exposed to sputtered species (-100 V, 5 mA/cm², 5 minutes), as well as on the substrate tube (-100 V, 5 mA/cm², 10 minutes). The tantalum portion of the target tube assembly was retracted into a protected area of the apparatus so that it was not exposed to material sputtered from the substrate tube and other components during ion cleaning. The stainless steel extension on the target thus served as a "catcher" for material removed from these components.

At the completion of the etch process, the tantalum portion of the target was moved into position and conditions were adjusted to those required for the sputtering run. Run times were chosen to produce coating thicknesses commonly used for gun bore applications (75 to 150 μm). Background gases were monitored during both the pre-run bakeout and the coating phase of the run by using a residual gas analyzer. At the completion of the coating run, the system was allowed to cool overnight before being vented with dry nitrogen for substrate removal.

A set of baseline coating conditions from which parameters were varied for evaluation included:

- 200°C substrate temperature
- Krypton sputtering gas
- ~4.5 Pa sputtering gas pressure
- -1500 V DC, 10 mA/cm² target
- -100 V DC, ~5 mA/cm² substrate

These baseline conditions were chosen because they combined high-coating deposition rates (~25 μm/hour), a dense coating microstructure, and primarily bcc phase deposition. Specific run condition parameters for the samples discussed in this report are summarized in Table 1.

Table I. Deposition Conditions and Properties of Thick Tantalum Coatings Produced Using a Cylindrical Triode-Sputtering Apparatus

Run #	Sputtering Gas	Substrate Bias (V)	Gas Pressure (Pa)	Substrate Temperature (°C)	Run Duration (hr)	Avg. Coating Thickness (μm) ^a	Growth Surface Phase ^b	Preferred Crystal Orientation ^b	Coating Microhardness (Avg. Knoop)
121	Ar ^c	-100	0.67	202-210	7.0	100	beta	none	813
132	Kr	-100	0.40	203-211	5.7	140	bcc	110	393
125	Xe	-100	0.40	184-188	4.5	150	bcc	110	301
147	Xe/Ar	-100	0.40/0.67	162-171 ^d	1.5/2.0	80	beta	222, 211, 321	312/677
146	Xe	-100	0.40	98-109	4.0	130	bcc	110	283
150	Kr	0	0.45	181-197	5.0	130	beta	002, 211	1166
155	Kr	-50	0.45	186-202	5.0	140	bcc	110	401
161	Kr	-100	0.45	202-205	5.0	120	bcc	110	376
152	Kr	-150	0.45	197-204	5.0	120	bcc	110 (weak)	387
163	Kr	0/-100	0.45	199-200	3.0/2.0	130	bcc	110	1129/349
158	Xe	50/30/0/100	0.40	199-202	1.0/1.0/1.0/1.0	140	bcc	110	1047/354

^aAverage coating thickness calculated based on substrate weight gain and assuming a coating density of bulk tantalum.

^bBy growth surface x-ray diffraction.

^cBold parameter indicates significant deviation from baseline conditions.

^dSample temperature for this run was ~30° lower than anticipated due to an error in machining the outer substrate diameter.

Coating Characterization

Coated cylinders were sectioned using a carbide cutoff wheel. Optical micrographs and Knoop microhardness diamond indentation measurements (100-g load) were taken on mounted and polished coating cross sections. The samples were subsequently acid etched to reveal the coating microstructure, and additional micrographs were taken. The phase distribution and preferred crystallographic orientation at the growth surface was established using a Scintag PTS2000 x-ray diffractometer operated with copper K-alpha radiation.

RESULTS AND DISCUSSION

Unless otherwise noted, the growth surfaces of the tantalum deposits described in this report were metallic gray in appearance and were smooth and reflective. Some samples also contained areas having a slightly hazy appearance, suggesting minor growth surface irregularities. All coatings appeared adherent to the substrate tube, and did not debond as a result of sectioning with an abrasive cutoff wheel. The crystallographic and metallographic analyses of the samples discussed below are included in Table 1.

We have previously demonstrated that, under otherwise similar baseline coating conditions, heavier sputtering gases (krypton, xenon) exhibited a stronger tendency to produce the bcc phase in thick sputtered tantalum coatings than the more commonly used sputtering gas, argon. This conclusion was supported by surface x-ray analysis and by microindentation measurements taken on cross-sectioned samples produced using the individual gases (ref 2). In addition to crystallographic phase differences, the coating microstructure was also affected by the use of the different sputtering gases. Figure 1 contains photomicrographs of acid-etched tantalum coatings produced using argon, krypton, and xenon under otherwise similar coating conditions. Distinct phase composition and microstructural differences were observed in the tantalum coating as a result of using the different gases. Specifically, the use of argon gas resulted in the formation of a primarily beta phase coating consisting of a porous columnar structure (Figure 1a). In contrast, the use of xenon gas produced a fine-grained, dense microstructure consisting exclusively of the bcc phase (Figure 1c). The sample deposited using krypton gas under these conditions (Figure 1b) was primarily fine-grained, dense bcc tantalum. However, the krypton-generated coating also contained some beta-phase material at the interface and in randomly spaced porous stringers extending through the bcc layer in the direction of the coating growth.

An additional sample (#147) was produced in which a first layer was deposited using xenon gas, followed immediately by deposition of a surface layer using argon. During the transition between the two gases (~2 minutes), the target voltage was turned off, the plasma was extinguished, and xenon was pumped out of the system and replaced by argon gas. A roughly 10°C drop in substrate temperature was noted during the gas changeover, but the equilibrium temperature was rapidly reestablished after resumption of sputtering with argon.

Figure 2 shows a photomicrograph of the acid-etched tantalum coating produced in the xenon/argon dual-gas run. In general, the microstructures observed in this coating were consistent with those produced using each gas independently (Figures 1a and 1c). Notably, the layer produced with argon retained a highly columnar microstructure, whereas the underlying layer produced with xenon was fine-grained and dense. Surface x-ray analysis and diamond microindentation hardness measurements confirmed the presence of the beta phase in the surface layer that was produced with argon. Microindentation hardness measurements and the observed dense microstructure were consistent with the formation of the bcc phase in the underlying coating produced with xenon.

Prior work had shown that when krypton was used as the sputtering gas in the tube sputtering apparatus, lower substrate temperatures tended to produce increasing concentrations of beta-tantalum (ref 2). A coating sample (#146) was produced using xenon gas and a low substrate temperature ($\sim 100^{\circ}\text{C}$) to determine whether the use of the heavier gas would produce similar results. Analysis of this sample indicated that the tantalum produced under these conditions was 100% fine-grained bcc phase (Figure 3), consistent with the microstructure of coatings produced using xenon at higher substrate temperatures but otherwise similar bias and deposition rate conditions (Figure 1c). Growth surface x-ray analysis and microindentation hardness measurements taken on the coating cross section confirmed the presence of a single-phase bcc coating in this sample.

A series of coating samples was produced using krypton-sputtering gas and the other baseline conditions summarized above, but with varying substrate biases (0 to -150 V). Higher substrate biases were not tested due to plasma instability in the sputtering apparatus at higher bias voltages. Under the range of bias conditions evaluated, the coating system ran well and the coating surface appearances were similar. Surface x-ray analysis and metallographic cross-section analysis indicated that all samples produced using substrate biases of 50 V or higher yielded coatings consisting primarily of the bcc phase, and that these coatings exhibited no significant variation in Knoop microhardness (Table 1). The coatings were also fine-grained, exhibiting no columnar growth features. Sample #150, produced with the substrate unbiased (electrically floating), yielded single-phase beta tantalum exclusively. In contrast with the beta-phase coatings produced using argon (Figures 1 and 2), however, this beta sample was fine-grained and dense. Cross-sectional micrographs of the series of etched tantalum coatings produced using krypton-sputtering gas, a 200°C substrate temperature, and various substrate biases are shown in Figure 4. The figure also shows growth surface x-ray patterns for this series of samples.

To confirm the effect of bias on the tantalum coating phase, a separate sample (#163) was produced using a stepped bias during the run. The initial phase of the coating was deposited without applied substrate bias, followed by a period of deposit with the substrate biased at -100 V. The transition from unbiased to biased condition was performed by simply turning on the substrate bias power supply during deposition. There was no interruption of the plasma conditions or the coating process during the transition. Cross-sectional analysis of the coating produced in this stepped bias run indicated a nearly exclusive fine-grained beta phase formation in the unbiased portion of the run, and primarily fine-grained bcc phase after application of the bias (Figure 5). The area of transition between beta and bcc phase was also characterized in some areas of the sample, by a longitudinal crack running parallel to the transition interface. The crack typically occurred on the beta side of the beta/bcc interface and likely resulted from differences in coating stress on either side of the phase transition. Similar cracks running parallel to the coating interface have been noted in other thick beta phase sputtered tantalum deposits (ref 1).

A tantalum-coated sample was also produced using xenon as the sputtering gas and a 200°C substrate temperature, while varying the bias in stages from 0 to -100 V during the sputtering run (#158). Figure 6 shows the microstructure of the resulting tantalum coating. The deposit produced during the first three hours of the run, at substrate biases of -50 V or less,

exhibited characteristic properties of the beta phase (e.g., high Knoop microhardness values, crack formation parallel to the interface). In contrast, the growth surface, which was deposited during the last hour of the run at -100 V bias, exhibited much lower Knoop microhardness values and exhibited no crack formation. Surface x-ray analysis confirmed that this surface layer consisted exclusively of the bcc phase.

Our results suggest that both the sputtering gas species and the bias applied to the growing tantalum film can significantly influence the phase and microstructure of the coating. These results can at least qualitatively be compared with the results obtained by Ino et al. (ref 9), who related the phase obtained in thin-sputtered tantalum films with the ion bombarding energy or ion momentum for argon and xenon species. Ino et al. showed that, for a normalized ion flux of 26 and on a silicon substrate, xenon gas produced the bcc phase within an ion bombardment energy window from roughly 30 to 90 eV. Higher and lower ion bombardment energies produced increasing concentrations of beta phase. When using argon as the sputtering gas, they found that the upper bias limit of the bcc-formation window was shifted to lower ion bombarding energy (~ 30 eV), and that a lower limit to the window was not detected at ion energies down to 5 eV. Although Ino et al. did not test krypton gas, we speculate that the bcc-formation window for that gas would have fallen between those of xenon and argon because of its intermediate mass.

The results of the study presented here are consistent with the general trends noted by Ino et al., although we speculate that positions of the bcc-formation windows for the different sputtering gases are shifted from the values reported by them due to differences in ion flux, substrate material, deposition rates, and deposition temperature. We suggest that the bcc-formation window under our deposition conditions still extends to the highest ion bombardment energy for xenon, to a lower value for krypton, and yet lower for argon. At a 100 V bias, the xenon- and krypton-deposited coatings fall within the bcc-window, while the 100 V bias falls beyond the upper limit of the bcc window for argon-deposited coatings. The results of the series of runs undertaken using krypton and different bias conditions indicate that, at the conditions used for this study, the lower limit for the bcc-window falls between 0 and 50 eV. The results from run #158 suggest that for xenon, the lower limit of the window must fall between 100 V and 50 V.

CONCLUSIONS AND FUTURE WORK

The results of this study indicate that both sputtering ion species and substrate bias during the deposition process strongly affect the phase and microstructure of thick sputtered tantalum coatings. With the cylindrical sputtering apparatus, a 200°C substrate temperature, a -1500 V target bias, and a -100 V substrate bias during the deposit, dense bcc phase tantalum was the primary product using either krypton or xenon sputtering gases. Using similar conditions, but with argon as the sputtering gas, a beta-phase tantalum coating having distinct columnar microstructure was produced. When using krypton sputtering gas and otherwise similar sputtering conditions, an unbiased substrate produced a beta-phase tantalum, but without the columnar growth structure. Samples produced at these conditions with higher substrate biases contained dense bcc-phase tantalum. Sputtered tantalum coatings produced with xenon gas at -100 V substrate bias were consistently bcc-phase, although use of xenon gas with substrate biases of -50 V or less produced beta-phase coatings. Coating phase and microstructure could be

altered in mid-run simply by adjusting the sputtering parameters, and were apparently not influenced by the structure or phase of the previously deposited material. The results obtained are consistent with the existence of bcc-phase formation "windows" whose positions depend on substrate bias and sputtering gas species. Future work in this area will include variable bias studies using argon-sputtering gas to confirm that it follows the same trends observed for xenon and krypton, and that thick bcc-phase coatings can be produced using this gas under the proper conditions.

REFERENCES

1. Matson, D.W., Merz, M.D., and McClanahan, E.D., *Journal of Vacuum Science and Technology A*, Vol. 10, 1992, p. 1791.
2. Matson, D.W., McClanahan, E.D., Rice, J.P., Lee, S.L., and Windover, D., *Surface and Coatings Technology*, Vol. 133-134, 2000, p. 411.
3. Lee, S.L., and Windover, D., *Surface and Coatings Technology*, Vol. 108-109, 1998, p. 65.
4. Cox, J.F., and McClanahan, E.D., in: *Proceedings of the Tri-Service Gun Tube Wear and Erosion Symposium*, 1982, p. 277.
5. Read, M.H., and Altman, C., *Applied Physics Letters*, Vol. 7, 1965, p. 51.
6. Feinstein, L.G., and Huttemann, R.D., *Thin Solid Films*, Vol. 16, 1973, p. 129.
7. Moseley, P.T., and Seabrook, C.J., *Acta Crystallographica, Section B*, Vol. 29, 1973, p. 1170.
8. Roy, R.A., Catania, P., Saenger, K.L., Cuomo, J.J., and Lossy, R.L., *Journal of Vacuum Science and Technology B*, Vol. 11, 1993, p. 1921.
9. Ino, K., Shinohara, T., Ushikai, T., and Ohmi, T., *Journal of Vacuum Science and Technology A*, Vol. 15, 1997, p. 2627.
10. Face, D.W., and Prober, D.E., *Journal of Vacuum Science and Technology A*, Vol. 5, 1987, p. 3408.
11. Westwood, W.D., Waterhouse, N., and Wilcox, P.S., *Tantalum Thin Films*, Academic Press, London, 1975.
12. Mattox, D.M., and Kominiak, G.J., *Journal of Vacuum Science and Technology*, Vol. 9, 1971, p. 528.
13. Heiber, K., and Mayer, N.M., *Thin Solid Films*, Vol. 90, 1982, p. 43.
14. Sato, S., *Thin Solid Films*, Vol. 94, 1982, p. 321.

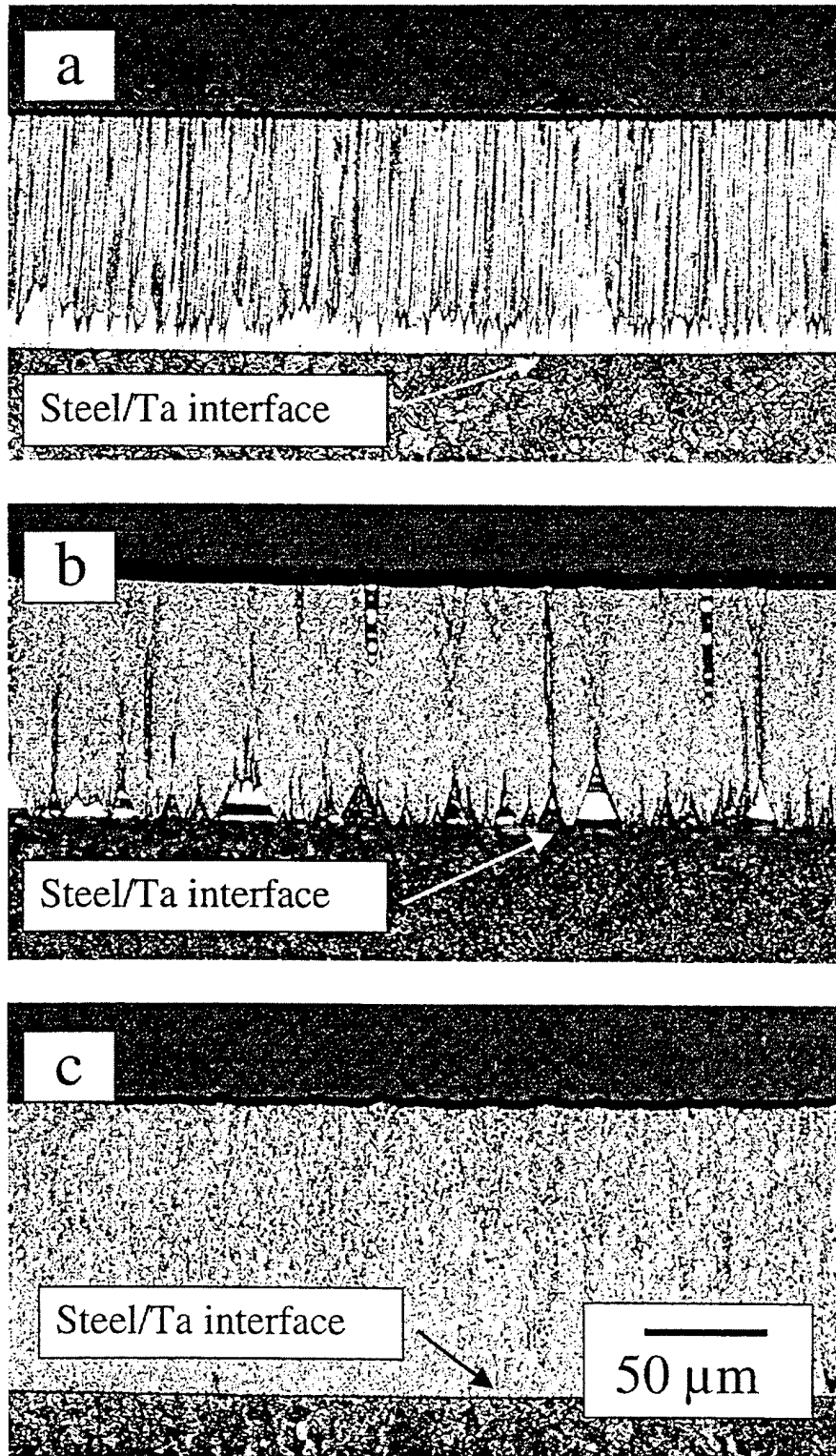


Figure 1. Photomicrographs of cross-sectioned and acid-etched tantalum coatings produced in the cylindrical triode-sputtering apparatus with a 200°C substrate temperature and -100 V substrate bias using (a) argon (#121), (b) krypton (#132), and (c) xenon (#125) sputtering gases.

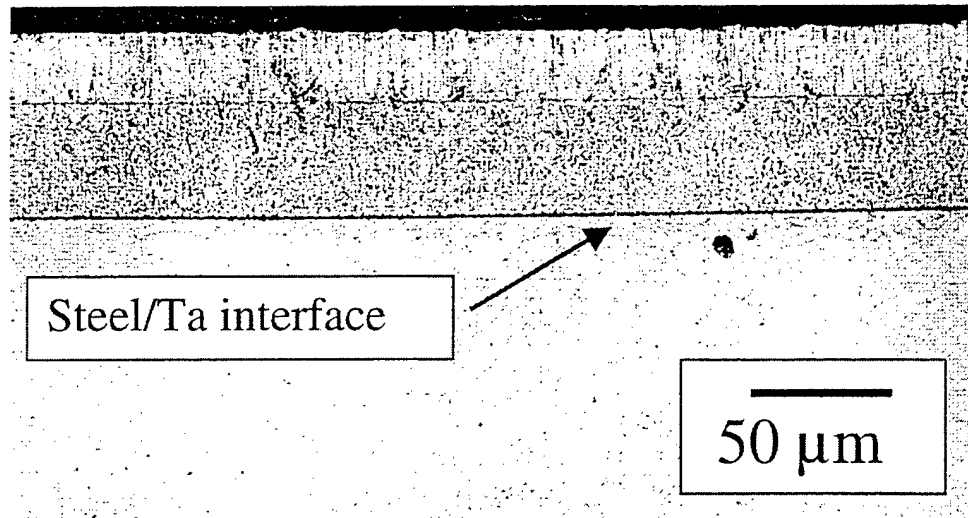


Figure 2. Photomicrograph of a cross-sectioned and acid-etched tantalum coating (sample #147) produced by sequential deposition with xenon and argon sputtering gases at $\sim 165^{\circ}\text{C}$ substrate temperature and a -100 V substrate bias.

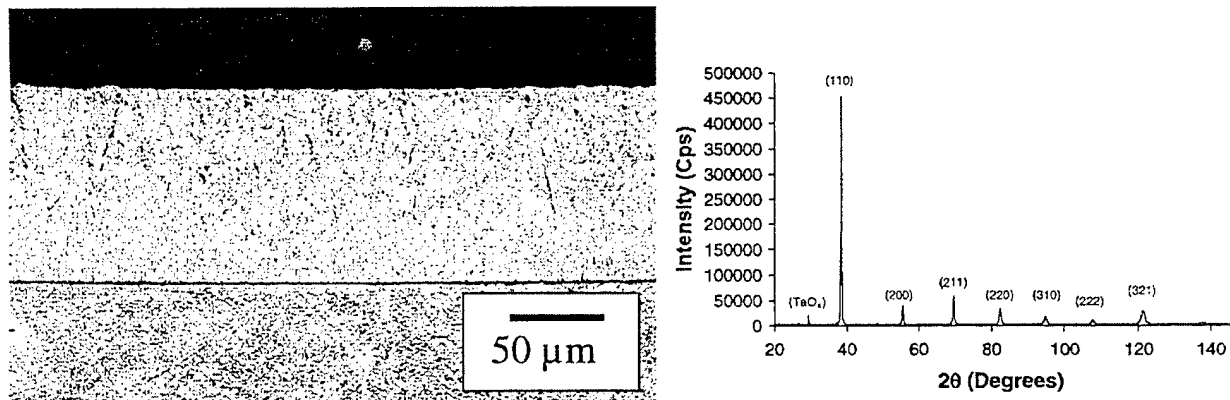


Figure 3. Photomicrograph and x-ray diffraction pattern of a tantalum coating (sample #146) produced using xenon gas, a 100°C substrate temperature, and -100 V substrate bias. The strong 110 crystallographic orientation is characteristic of the bcc phase.

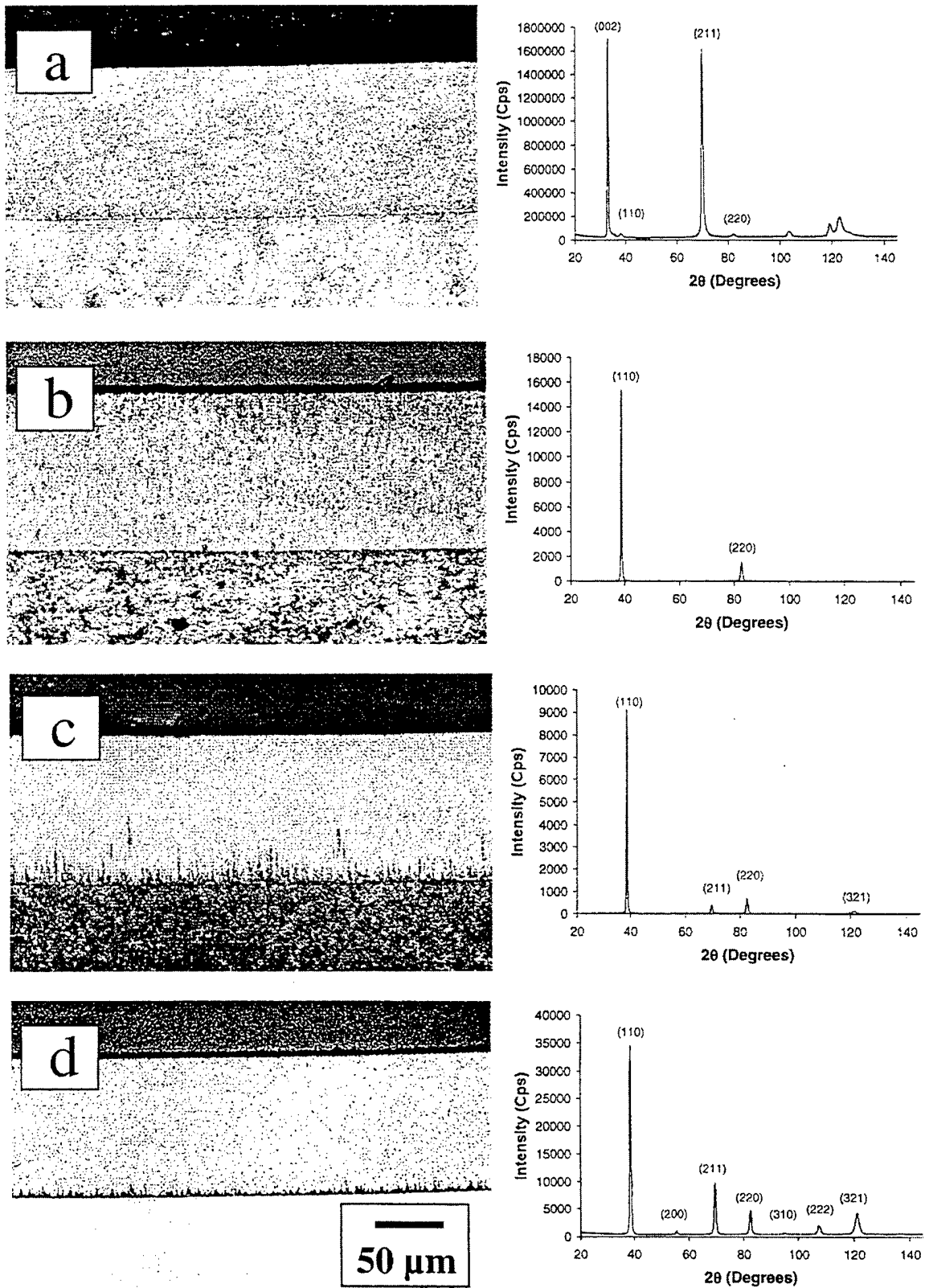


Figure 4. Photomicrographs of tantalum coatings produced using krypton sputtering gas, a 200°C substrate temperature, and various substrate biases including (a) floating (#150), (b) -50 V (#155), (c) -100 V (#161), and (d) -150 V (#152). A surface x-ray diffraction pattern for each sample is shown to the right of each photomicrograph.

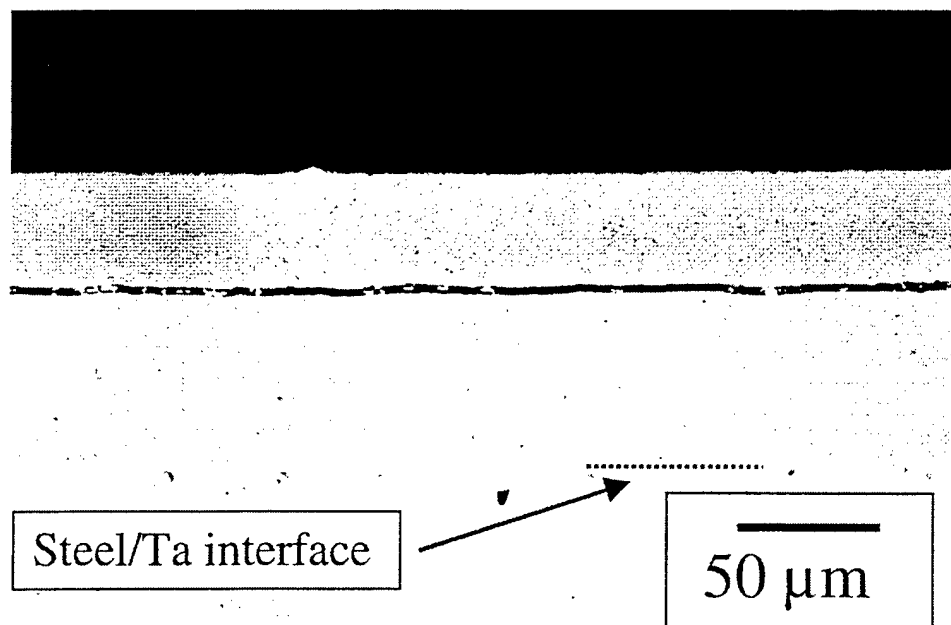


Figure 5. Photomicrograph of a sputtered tantalum sample (#163) produced using krypton sputtering gas, a 200°C substrate temperature, and a stepped substrate bias (initially unbiased, -100 V in the outer layer). The irregular dark line at about two-thirds of the coating thickness is a crack near the outer limit of the continuous beta phase.

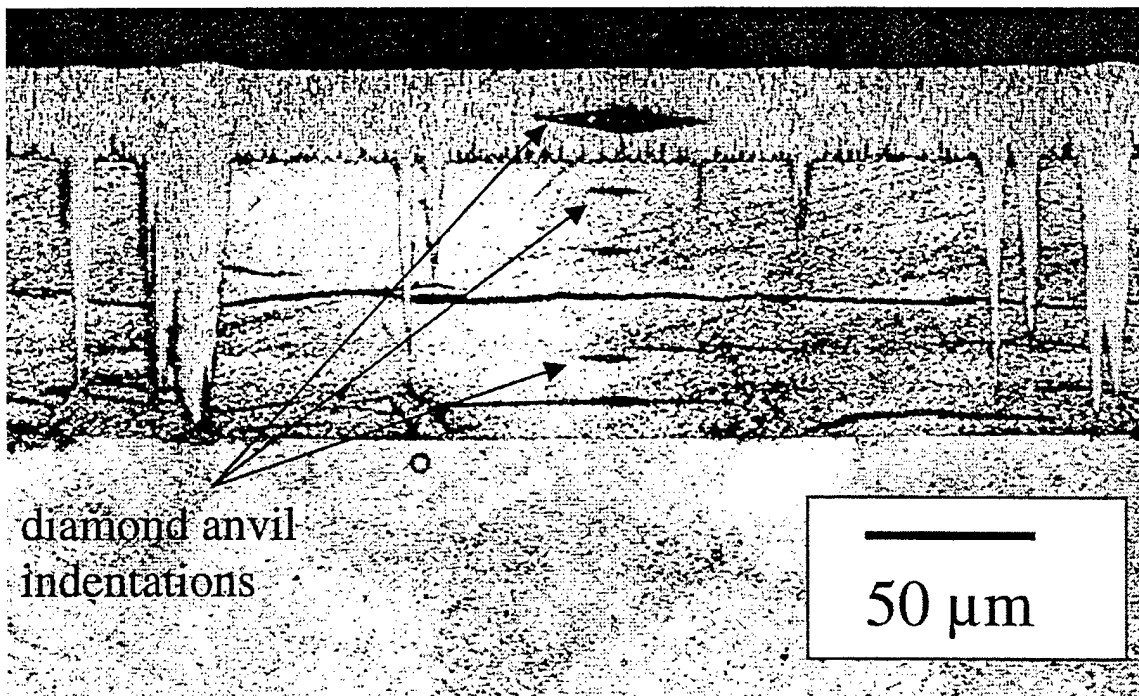
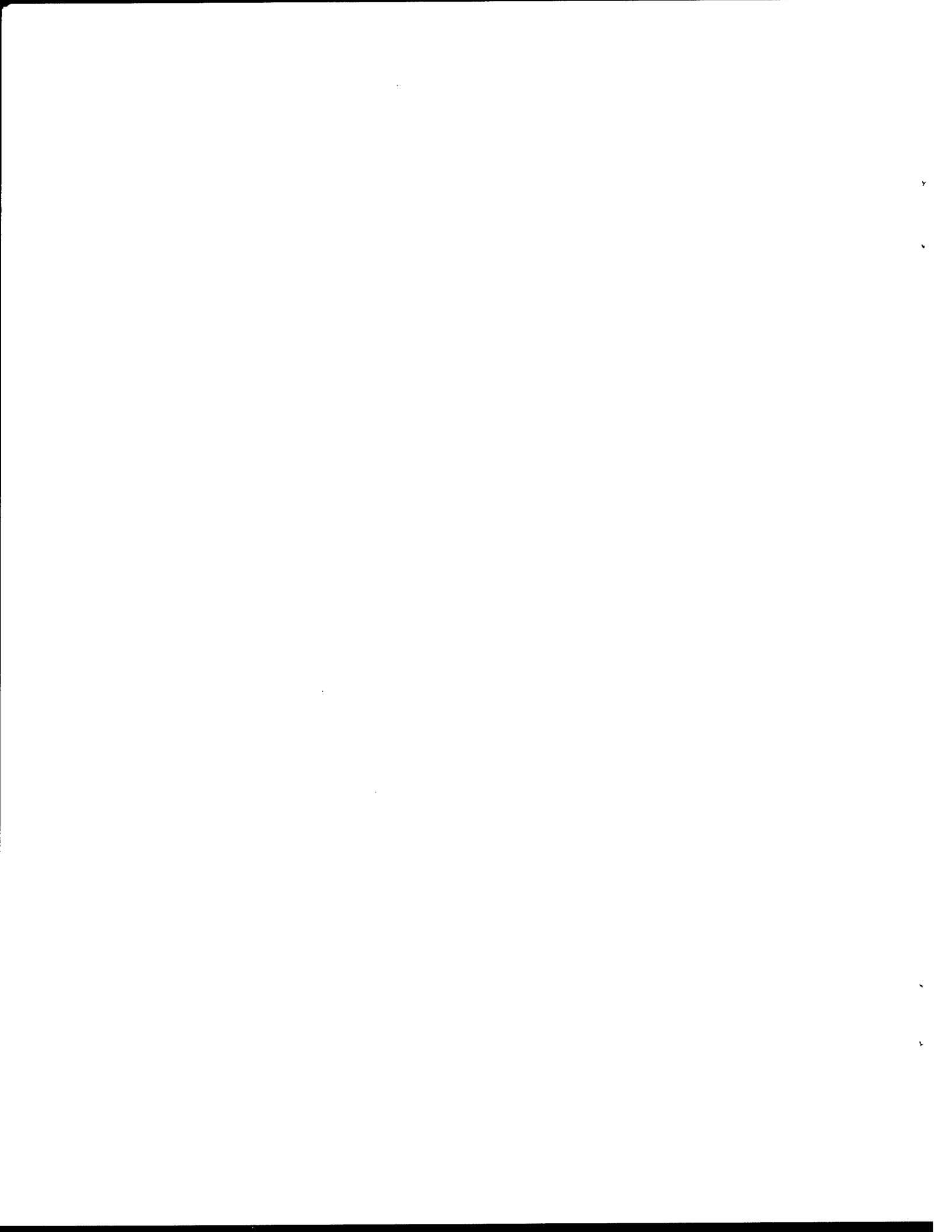


Figure 6. Photomicrograph of a cross-sectioned, sputtered tantalum coating (sample #158) produced using xenon gas, a 200°C substrate temperature, and various substrate biases (0 to -50 V for the deposit closest to the steel interface and -100 V for the outer layer). Diamond indentations indicate the relative hardness of the inner layers produced at low bias compared with the outer layer produced at -100 V bias.



TECHNICAL REPORT INTERNAL DISTRIBUTION LIST

	<u>NO. OF COPIES</u>
TECHNICAL LIBRARY ATTN: AMSTA-AR-CCB-O	5
TECHNICAL PUBLICATIONS & EDITING SECTION ATTN: AMSTA-AR-CCB-O	3
OPERATIONS DIRECTORATE ATTN: SIOVV-ODP-P	1
DIRECTOR, PROCUREMENT & CONTRACTING DIRECTORATE ATTN: SIOVV-PP	1
DIRECTOR, PRODUCT ASSURANCE & TEST DIRECTORATE ATTN: SIOVV-QA	1

NOTE: PLEASE NOTIFY DIRECTOR, BENÉT LABORATORIES, ATTN: AMSTA-AR-CCB-O OF ADDRESS CHANGES.

TECHNICAL REPORT EXTERNAL DISTRIBUTION LIST

	<u>NO. OF COPIES</u>		<u>NO. OF COPIES</u>
DEFENSE TECHNICAL INFO CENTER ATTN: DTIC-OCA (ACQUISITIONS) 8725 JOHN J. KINGMAN ROAD STE 0944 FT. BELVOIR, VA 22060-6218	2	COMMANDER ROCK ISLAND ARSENAL ATTN: SIORI-SEM-L ROCK ISLAND, IL 61299-5001	1
COMMANDER U.S. ARMY ARDEC ATTN: AMSTA-AR-WEE, BLDG. 3022 AMSTA-AR-AET-O, BLDG. 183 AMSTA-AR-FSA, BLDG. 61 AMSTA-AR-FSX AMSTA-AR-FSA-M, BLDG. 61 SO AMSTA-AR-WEL-TL, BLDG. 59 PICATINNY ARSENAL, NJ 07806-5000	1 1 1 1 1 2	COMMANDER U.S. ARMY TANK-AUTMV R&D COMMAND ATTN: AMSTA-DDL (TECH LIBRARY) WARREN, MI 48397-5000 COMMANDER U.S. MILITARY ACADEMY ATTN: DEPT OF CIVIL & MECH ENGR WEST POINT, NY 10966-1792	1
DIRECTOR U.S. ARMY RESEARCH LABORATORY ATTN: AMSRL-DD-T, BLDG. 305 ABERDEEN PROVING GROUND, MD 21005-5066	1	U.S. ARMY AVIATION AND MISSILE COM REDSTONE SCIENTIFIC INFO CENTER ATTN: AMSAM-RD-OB-R (DOCUMENTS) REDSTONE ARSENAL, AL 35898-5000	2
DIRECTOR U.S. ARMY RESEARCH LABORATORY ATTN: AMSRL-WM-MB (DR. B. BURNS) ABERDEEN PROVING GROUND, MD 21005-5066	1	COMMANDER U.S. ARMY FOREIGN SCI & TECH CENTER ATTN: DRXST-SD 220 7TH STREET, N.E. CHARLOTTESVILLE, VA 22901	1
COMMANDER U.S. ARMY RESEARCH OFFICE ATTN: TECHNICAL LIBRARIAN P.O. BOX 12211 4300 S. MIAMI BOULEVARD RESEARCH TRIANGLE PARK, NC 27709-2211	1		

NOTE: PLEASE NOTIFY COMMANDER, ARMAMENT RESEARCH, DEVELOPMENT, AND ENGINEERING CENTER,
BENÉT LABORATORIES, CCAC, U.S. ARMY TANK-AUTOMOTIVE AND ARMAMENTS COMMAND,
AMSTA-AR-CCB-O, WATERVLIET, NY 12189-4050 OF ADDRESS CHANGES.
